

Supplementary Materials for

Anti-VEGF therapy induces ECM remodeling and mechanical barriers to therapy in colorectal cancer liver metastases

Nuh N. Rahbari, Dmitriy Kedrin, Joao Incio, Hao Liu, William W. Ho, Hadi T. Nia, Christina M. Edrich, Keehoon Jung, Julien Daubriac, Ivy Chen, Takahiro Heishi, John D. Martin, Yuhui Huang, Nir Maimon, Christoph Reissfelder, Jurgen Weitz, Yves Boucher, Jeffrey W. Clark, Alan J. Grodzinsky, Dan G. Duda, Rakesh K. Jain*, Dai Fukumura*

*Corresponding author. Email: dai@steele.mgh.harvard.edu (D.F.); jain@steele.mgh.harvard.edu (R.K.J.)

Published 12 October 2016, *Sci. Transl. Med.* **8**, 360ra135 (2016)

DOI: 10.1126/scitranslmed.aaf5219

This PDF file includes:

Materials and Methods

Fig. S1. Expression of HA is increased in CRC liver metastases compared to liver parenchyma.

Fig. S2. DNA content in murine CRC liver metastases is decreased after anti-VEGF therapy.

Fig. S3. CD44 expression is increased in liver metastases after anti-VEGF therapy.

Fig. S4. Bevacizumab increases sGAG expression in human CRC liver metastases.

Fig. S5. Anti-VEGF therapy does not alter ECM expression in healthy liver parenchyma.

Fig. S6. Anti-VEGF therapy results in recruitment of MDSCs into CT26 liver metastases.

Fig. S7. Anti-VEGF therapy does not alter IM and neutrophil counts in the bone marrow.

Fig. S8. *Agtr1a* knockout does not alter anti-VEGF-induced tumor stiffness and expression of noncollagenous matrix.

Fig. S9. Anti-VEGF therapy does not increase TGF- β 1 expression in CRC liver metastases.

Fig. S10. Microvessel density is decreased, and hypoxia is increased in CT26 liver metastases after anti-VEGF therapy.

Fig. S11. Treatment with PEG-HAse lowers HA content in SL4 liver metastases.
Table S1. Clinicopathologic data of patients with CRC liver metastases.
Reference (78)

Supplementary Materials and Methods

ANIMALS: Male 8-10 week old wild-type C57BL/6 and BALB/c mice, as well as *Ccr2*^{-/-} and *Agtr1a*^{-/-} mice (78) were used. Mice were purchased from Jackson Laboratory (The Jackson Laboratory, Bar Harbor, Maine), bred and maintained in our defined-flora animal colony and used under NIH guidelines and IACUC approval. Animal studies were performed in accordance with the policies of the Massachusetts General Hospital subcommittee on Research Animal Care, according to approved animal use protocols.

CELLS AND CELL CULTURE: Cell line authentication and mycoplasma testing were performed on all cell lines. SL4 cells were cultured in DMEM / F12 1:1 mixture medium, CT26 cells were cultured in DMEM, and both were supplemented with 10% fetal bovine serum (FBS). HSC cells were cultured in Stellate Cell Medium (SteCM) supplemented with 2% FBS and 1% of stellate cell growth supplement (SteCGS). For in vivo experiments, SL4 and CT26 cells were harvested at ~70% confluency, washed twice with phosphate buffered saline (PBS), counted, and resuspended in Hanks' Balanced Salt solution (HBSS).

HYPOXIA AND STARVATION: Cells were cultured in 6-well plates and pre-starved for 12 hours in medium supplemented with 0.1% FBS. The medium was replaced with fresh starvation medium, and cell plates were placed into a hypoxia chamber (1% O₂) or regular cell culture chamber (21% O₂) for 48 hours.

LIVER METASTASIS MODEL: Mice were anesthetized with an intraperitoneal (i.p.) injection of ketamine (100 mg/kg) and xylazine (10 mg/kg). Aseptic technique was used for the entire duration of the procedure. A left flank incision was made through the skin and abdominal wall layer, and the spleen was gently exteriorized. The middle of the spleen was ligated with a suture before transection, with the goal of preserving the vascular pedicles to both created 'lobes'. 1x10⁵ cells in 100 μL serum-free medium were injected slowly into the caudal sector with a 30-gauge needle. After 10 minutes, the hemispleen used for tumor cell injection was resected. The remaining spleen was placed back into the abdomen. Abdominal

wall was closed with a continuous suture. The skin was closed with surgical staples. Treatments were initiated after of the mice developed macroscopically visible liver metastases (~ 8-12 days after injection).

ASSESSMENT OF TUMOR BURDEN:

Blood Gaussia Luciferase (Gluc) assay: SL4 cells were stably transduced with a lentivirus encoding the *Gluc* gene (73). Blood Gluc activity in tumor-bearing mice was measured as described previously (74). In brief, 13 μ L of whole blood was collected in an EDTA-containing tube from the tail vein of the tumor-bearing mice twice a week. Blood Gluc activity was measured using a diluted Coelenterazine (Nanolight, Cat#303-10) solution (1:100) and a GloMax 96 Microplate Luminometer (Promega).

Ultrasound imaging: Mice were anesthetized with isoflurane. After hair removal, ultrasound imaging of the liver was carried out with the Vevo 2100 system (VisualSonic) with MS550S 40 MHz probe. The measurements were gathered at least twice a week.

PEGYLATED HYALURONIDASE SYNTHESIS: Hyaluronidase (rhuPH20, Hylenex, Halozyme Therapeutics or hyaluronidase from bovine testes, Sigma-Aldrich) was coupled to a succinimidyl ester (NHS) activated PEG derivative (mPEG-NHS-30K, Nanocs) at a PEG:polypeptide molar ratio of 10:1 in a buffer solution containing phosphate-buffered saline (PBS, pH 7.4) and 0.1 M borate (pH 8.5). The mixture was stirred at 4°C for 2 hours to allow coupling reaction. The resulting PEGylated protein was purified and free PEG was removed by ultrafiltration.

TREATMENTS: Mice bearing established liver metastases were randomly allocated to the treatment groups. The anti-VEGF monoclonal antibody B20.4-1.1 (Genentech) was administered by intraperitoneal (i.p.) injection twice a week at 5 mg/kg or 1 mg/kg. For depletion of metastasis-associated neutrophils, an anti-Ly6G antibody (clone RB6-8C5; BioXcell) was administered i.p. every 2 days at a dose of 5 mg/kg. Pegylated hyaluronidase (PEGHase) was administered by tail vein injection twice a week or 24 hours before administration of chemotherapy at a dose of 4.5 mg/kg (43). Chemotherapy with 5-fluorouracil (APP Pharmaceuticals, LLC) was administered intravenously twice a week by retroorbital injection at a dose of 50 mg/kg. Mice were treated until moribund, unless indicated otherwise.

TISSUE AND BLOOD SAMPLING: After excision of the entire liver, one tumor-bearing lobe was used to collect tumor tissue for further analyses (biochemical analyses, qRT-PCR, flow cytometry, tumor stiffness). Remaining tumor-bearing lobes were fixed in 4% paraformaldehyde (PFA) overnight, then prepared for paraffin embedding for further analysis. Blood samples were collected by cardiac puncture. Spleens were collected for flow cytometry in cold HBSS. For collection of the bone marrow, one femur per mouse was flushed with 200 μ l PBS.

IMMUNOHISTOCHEMISTRY: Snap frozen tumor samples were embedded in OCT compound (Sakura). Frozen blocks were kept at -80°C and cut at 20 μ m thickness for immunofluorescence staining. The following antibodies were used: SMA (C6198 antibody, Sigma), collagen-I (LF-68 antibody, provided by Dr. Larry Fisher, NIDCR), hyaluronan (biotinylated hyaluronan proteoglycan fragment; 385911, Calbiochem), pimonidazole (Hypoxyprobe-1 MAb1, Hypoxyprobe, Inc.). Samples were counterstained with 40,6-diamidino-2-phenylindole (DAPI, Vector Labs). Whole tumor mosaic images were obtained from each sample with an Olympus (FV1000) confocal laser-scanning microscope.

Paraffin-embedded tissue blocks were cut at 5 μ m thickness. Slides were stained with hematoxylin and eosin (H&E) or with antibodies to CD34 (Abcam, catalog# ab81289) or CD44 (eBioScience, catalog# 14-0441-85). For hypoxia staining, 60 mg/kg of pimonidazole hydrochloride was injected i.p. (Hypoxyprobe; Hypoxyprobe, Inc.) Mice were euthanized 60 minutes after injection, and tissue was collected for analysis as described above. After blocking with mouse IgG (M.O.M. Basic Kit #BMK2202; Vector Labs), pimonidazole antigens were stained with the mouse Ig monoclonal antibody, Hypoxyprobe-1 MAb1 (Hypoxyprobe, Inc.). Patient samples were stained for hyaluronan using a biotinylated hyaluronan proteoglycan fragment (Catalog #385911, Calbiochem). Image analyses were carried out in an automated fashion using a custom algorithm in MATLAB (The MathWorks).

FLOW CYTOMETRY: Tumor samples were excised, cut into small pieces, and incubated for 45 minutes in digestion medium containing collagenase type 1A (1.5 mg/mL; Sigma Aldrich), hyaluronidase (1.5 mg/mL, Sigma Aldrich), and DNase (20 U/mL, Sigma Aldrich). Samples were filtered through 70- μ m cell strainers, washed with flow cytometry staining buffer (containing 1% bovine serum albumin and

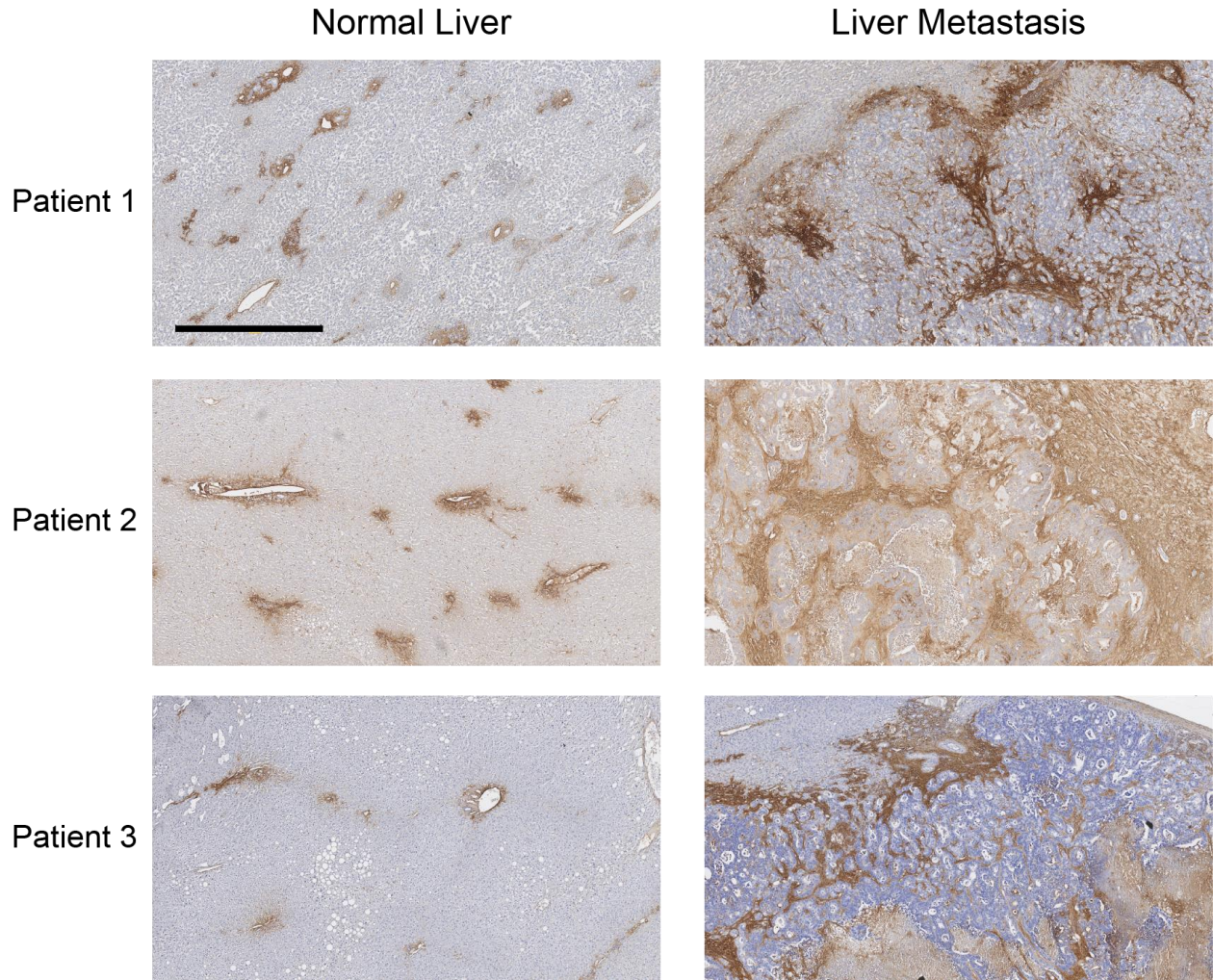
0.1% sodium azide), and filtered through 40- μ m cell strainers. After red blood cell lysis, blood samples were washed twice with flow cytometry staining buffer and filtered through 40- μ m cell strainers. Spleens were chopped and strained through 70- μ m cell strainers. After red blood cell lysis, spleen samples were washed twice with flow cytometry staining buffer and filtered through 40- μ m cell strainers to obtain a single cell suspension. Bone marrow samples were also filtered through 70- μ m cell strainers, washed with flow cytometry staining buffer, and filtered through 40- μ m cell strainers. Single cells were stained with the following monoclonal antibodies: PE-Cy7-CD45 (clone 30-F11), APC-Cy7-CD11b (clone M1/70), PE-Ly6C (clone HK1.4), FITC-Ly6G (clone 1A8) (all from BD Biosciences). Flow cytometry was performed after adding the nucleic acid dye 7-aminoactinomycin D (7-AAD; BD Pharmingen, Becton Dickinson) for exclusion of non-viable cells using an LSRII flow cytometer (Becton Dickinson).

DETERMINATION OF SULFATED GAG AND COLLAGEN CONTENT: The biochemical analyses for sulfated GAG and collagen content were performed on tumors of 5–10 mm diameter. Tumor tissues were rapidly frozen in liquid nitrogen and stored at -80°C . Each piece (40–50 mg for mouse samples and 17 – 150 mg for human samples) was weighed and then used for one of the two analyses. GAG content was determined by a previously described method (75). Tissues were finely dispersed with a homogenizer, solubilized in 1 ml of digestion buffer (125 $\mu\text{g}/\text{ml}$ papain in 0.1 M sodium phosphate, 5 mM $\text{Na}_2\text{-EDTA}$, and 5 mM cysteine-HCl, pH 6.0), and incubated for 18 hours at 60°C . Sulfated GAG content was determined with the Blyscan Proteoglycan and Glycosaminoglycan assay (Biocolor Ltd.). To measure total collagen content, 100 μl of papain digest were hydrolyzed in 6 N HCl at 110°C for 18 hours. The hydroxyproline content of the hydrolysate was then assessed by colorimetry (76). Results are expressed as mg of collagen by reference to a standard solution of purified collagen type I (Vitrogen 100; Collagen Corp.) in which hydroxyproline:collagen ratio of 6.8 was measured (77).

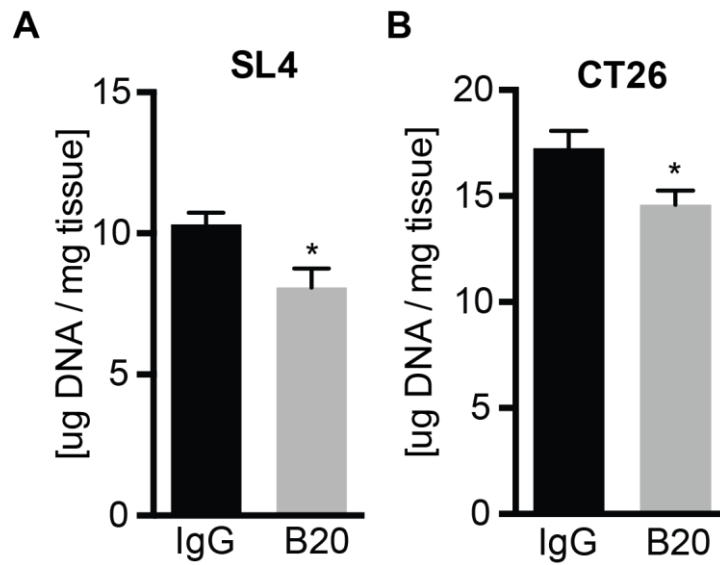
ELISA: Snap frozen tumor samples were homogenized, and protein was extracted using RIPA buffer supplemented with protease inhibitors (Roche) and phosphatase inhibitor cocktail (Sigma). Mouse HA and TGF- β 1 were quantified using ELISA kits according to the manufacturer's instructions (R&D Systems).

MEASUREMENT OF STIFFNESS AND SOLID STRESS: The stiffness (Young's modulus) of tumors was determined by unconfined compression tests (78). Slices of freshly excised tissue, 3 mm in diameter and ~ 2-mm thick, were placed in an unconfined compression chamber and submerged in physiological saline. The chamber was mounted in an ultrasensitive servo-controlled materials tester (Dynastat Mechanical Spectrometer; IMASS). Each specimen was compressed by 5 percent of the original height in ramps of 15 s and allowed to relax for 20 min. Four successive measurements were performed on each tissue slice. Solid stress was determined using a recently proposed method (6). In line with this method, the normalized tumor opening was used as a readout for growth-induced stress. Metastases were cut along their longest axis for about 80% of their thickness. Then the tumor opening, which is the gap between the two hemispheres at the surface of the tumor was measured with a caliper 10 minutes after the cut was made and was considered to be a global reflection of the circumferential tension at the tumor margin and intratumoral compressive forces.

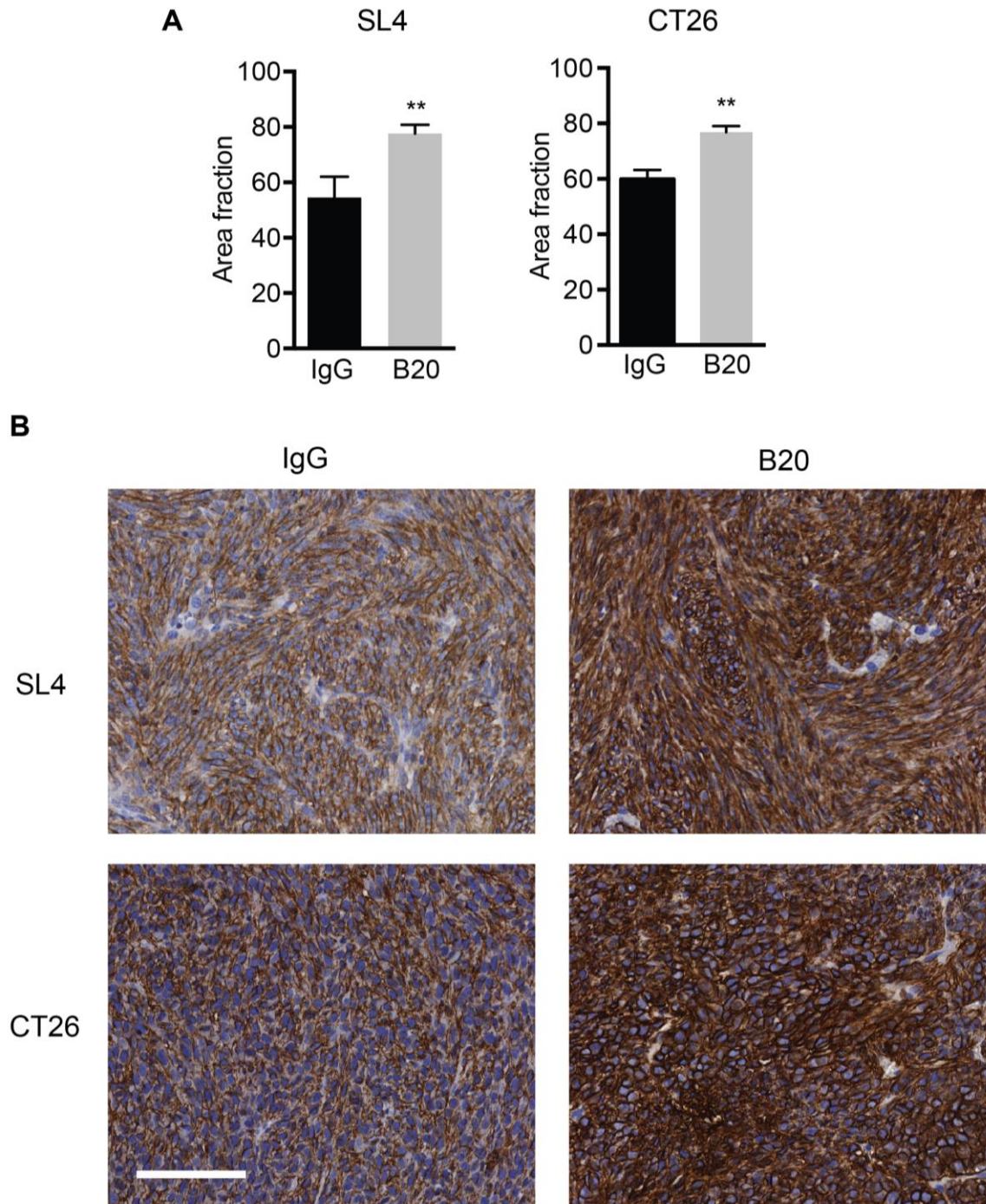
PERFUSION MEASUREMENT: Cannulation of a mesenteric vein was carried out with a 30-gauge needle. The perfusion marker Hoechst 33342 (Sigma Chemical Co.) was injected. The tumor samples were harvested 5 minutes after portal infusion of Hoechst 33342 and snap frozen. Measurement of tumor perfusion was then carried out as described previously (31).



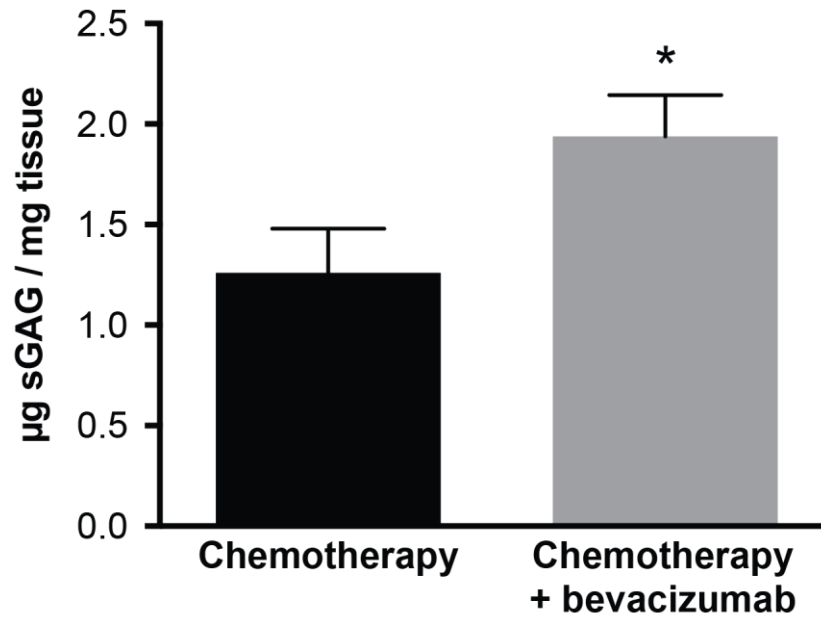
Supplementary Figure S1: Expression of HA is increased in CRC liver metastases compared to liver parenchyma. Samples from colorectal liver metastases and the corresponding liver parenchyma were obtained from the same patients. Scale bar 200 μ m.



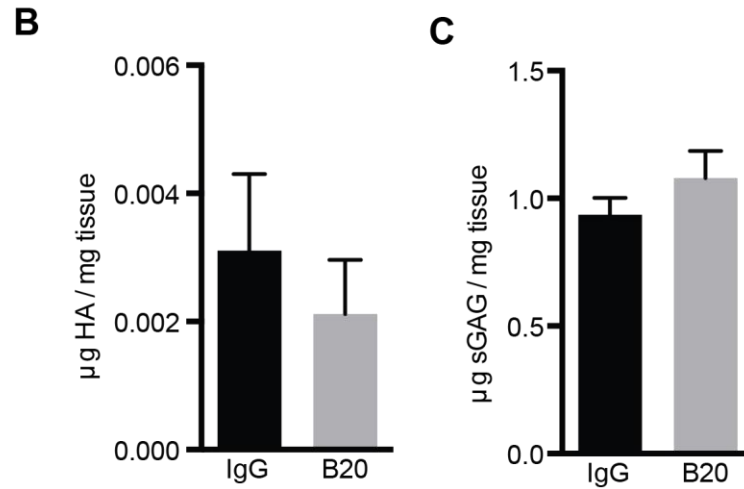
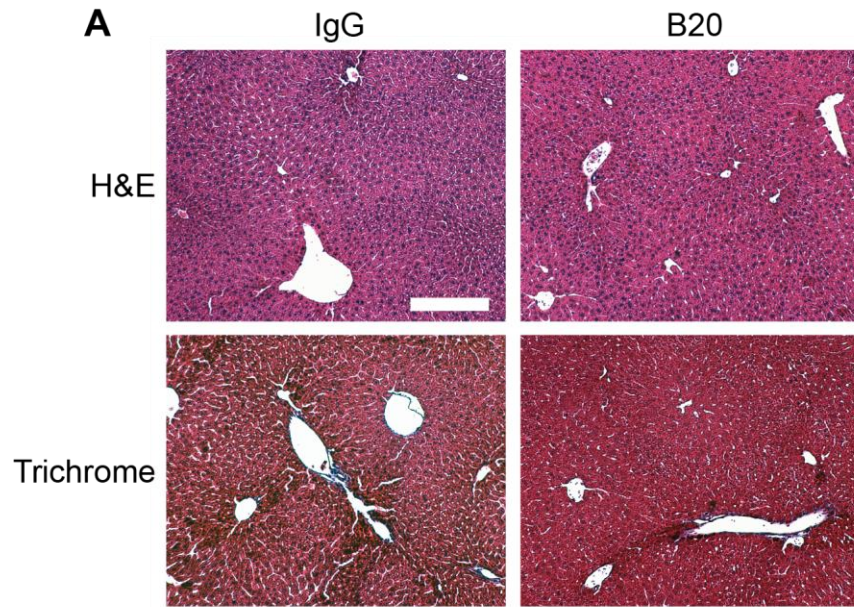
Supplementary Figure S2: DNA content in murine CRC liver metastases is decreased after anti-VEGF therapy. (A-B) Mice bearing SL4 ($*P = 0.011$, Student's t-test, $n = 8-9$ /group) (A) and CT26 ($*P = 0.011$, Student's t-test, $n = 9-10$ /group) (B) liver metastases were treated with either B20 or control IgG. Metastases were harvested when mice were moribund.



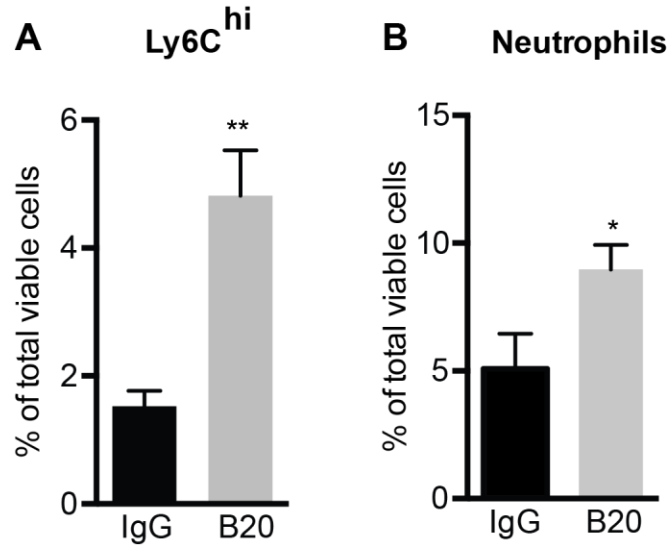
Supplementary Figure S3: CD44 expression is increased in liver metastases after anti-VEGF therapy. (A) Quantification of CD44 expression in SL4 (** $P = 0.008$; Student's t-test) and CT26 (** $P = 0.005$; Student's t-test) liver metastases grown in C57BL/6 and BALB/c WT mice after 6 days of treatment with IgG or B20 ($n = 4-9$ /group). (B) Representative immunohistochemistry images of CD44 expression in SL4 and CT26 liver metastases grown in C57BL/6 and BALB/c WT mice after 6 days of treatment with IgG or B20. Mice were treated with B20 (5 mg/kg) on day 0 and day 3. Scale bar 100 μm .



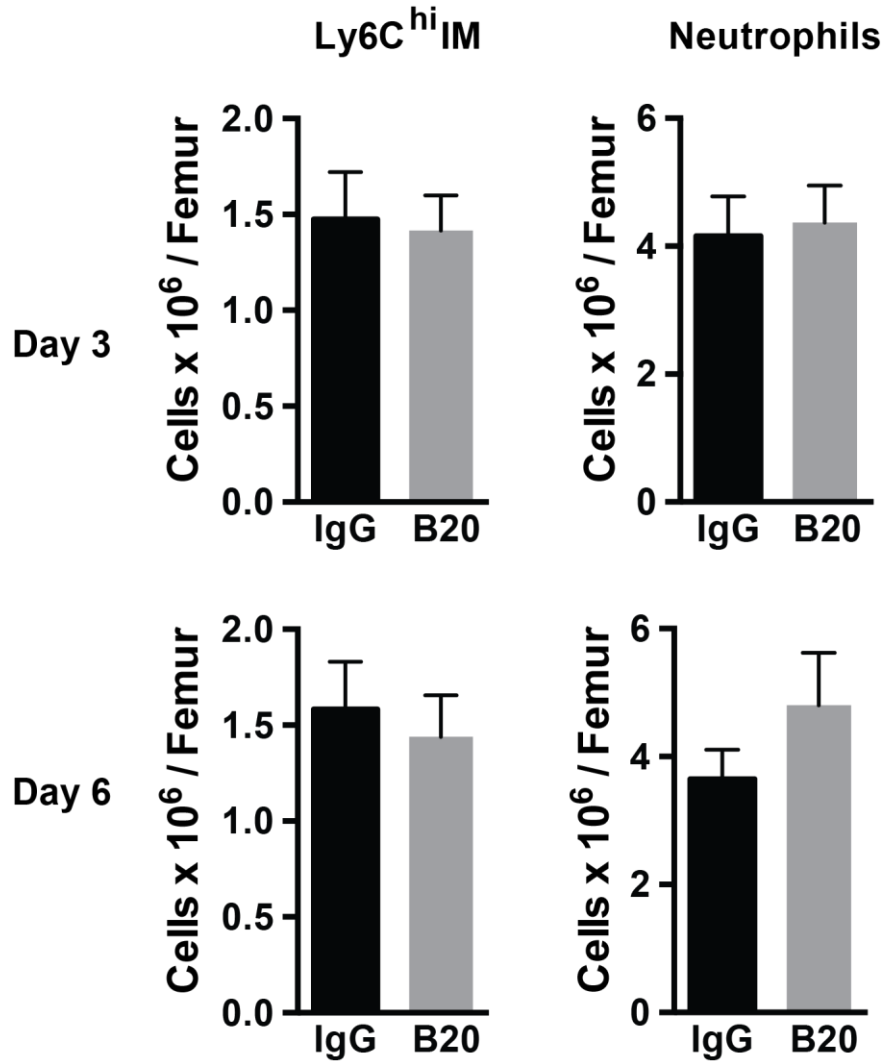
Supplementary Figure S4: Bevacizumab increases sGAG expression in human CRC liver metastases. Quantification of sGAG concentration by DMMB assay in human colorectal cancer liver metastases after preoperative systemic chemotherapy with and without bevacizumab (* $P = 0.035$, Student's t-test, $n = 10-11$ /group).



Supplementary Figure S5: Anti-VEGF therapy does not alter ECM expression in healthy liver parenchyma. Healthy non-tumor-bearing C57BL/6 mice were treated with either B20 or control IgG for 21 days. **(A)** Representative H&E and Masson-Trichrome staining of livers harvested from mice after completion of therapy. Scale bar 100 μ m. **(B)** Quantification of HA concentration in liver parenchyma by ELISA ($P = 0.504$, Student's t-test, $n = 4-6$ /group). **(C)** Quantification of sGAG concentration by DMMB assay ($P = 0.302$, Student's t-test, $n = 5-6$ /group).



Supplementary Figure S6: Anti-VEGF therapy results in recruitment of MDSCs into CT26 liver metastases. (A-B) FACS analysis of Ly6C^{hi} inflammatory monocytes (**P* = 0.006, Student's t-test, n = 5-9/group) (A) and metastasis-associated neutrophils (**P* = 0.037, Student's t-test, n = 5-9/group) (B) in CT26 liver metastases grown in BALB/c WT mice after 6 days of treatment with IgG or B20 (5 mg/kg, twice a week).



Supplementary Fig. S7: Anti-VEGF therapy does not alter IM and neutrophil counts in the bone marrow.

FACS analysis of Ly6C^{hi} inflammatory monocytes and neutrophils in the bone marrow of C57BL/6 WT mice bearing SL4 liver metastases after 3 days (Ly6C^{hi} IMs: $P = 0.852$; MANs: $P = 0.813$; Student's t-test) and 6 days (Ly6C^{hi} IMs: $P = 0.678$; MANs: $P = 0.216$; Student's t-test) of treatment with IgG or B20 ($n = 5-10$ /group). B20 treatments (5 mg/kg): on day 0 for 3-day experiments; on day 0 and day 3 for 6-day experiments.

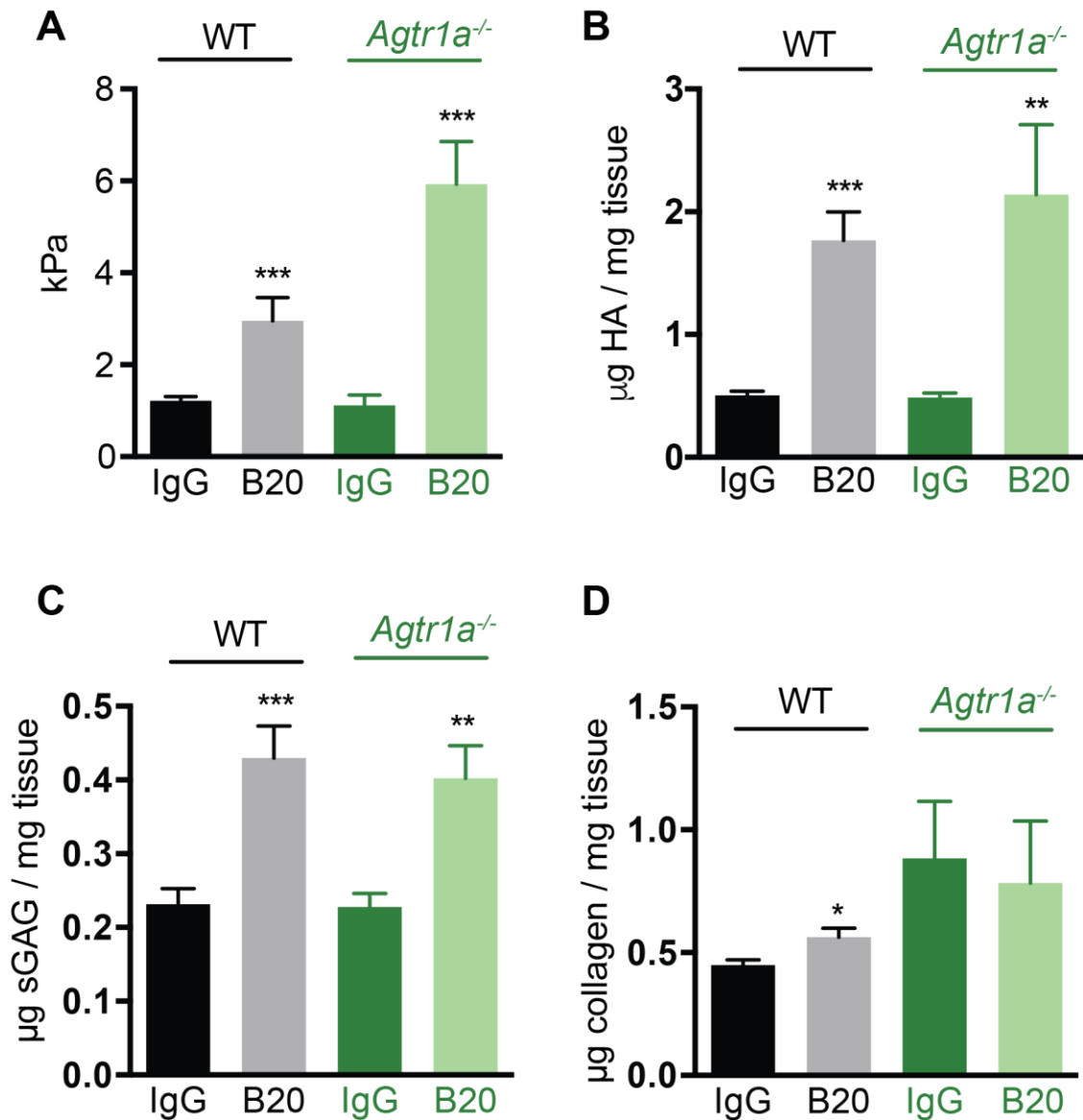


Fig. S8: *Agtr1a* knockout does not alter anti-VEGF-induced tumor stiffness and expression of noncollagenous matrix. C57BL/6 wild type mice (WT) and *Agtr1a*^{-/-} mice bearing established SL4 liver metastases were treated with either B20 (5 mg/kg, twice a week) or control IgG until moribund. **(A)** Stiffness measurements using unconfined compression tests of SL4 liver metastases in WT (***) $P = 0.001$, Student's t-test, $n = 9-12$ /group) and *Agtr1a*^{-/-} mice (***) $P = 0.0002$, Student's t-test, $n = 5-7$ /group). **(B)** Quantification of HA concentration in SL4 liver metastases by ELISA in WT (***) $P < 0.0001$, Student's t-test, $n = 12$ /group) and *Agtr1a*^{-/-} mice (***) $P = 0.008$, Student's t-test, $n = 3-5$ /group). **(C)** Quantification of sGAG concentration in SL4 liver metastases by DMMB assay in WT (***) $P = 0.0005$, Student's t-test, $n = 8-10$ /group) and *Agtr1a*^{-/-} mice (***) $P = 0.005$, Student's t-test, $n = 4-5$ /group). **(D)** Quantification of collagen in SL4 liver metastases by hydroxyproline assay in WT (*) $P = 0.01$, Student's t-test, $n = 6-10$ /group) and *Agtr1a*^{-/-} mice ($P = 0.776$, Student's t-test, $n = 4-5$ /group). Data from WT mice are from the same experiments presented in Figures 2B and 3A-C.

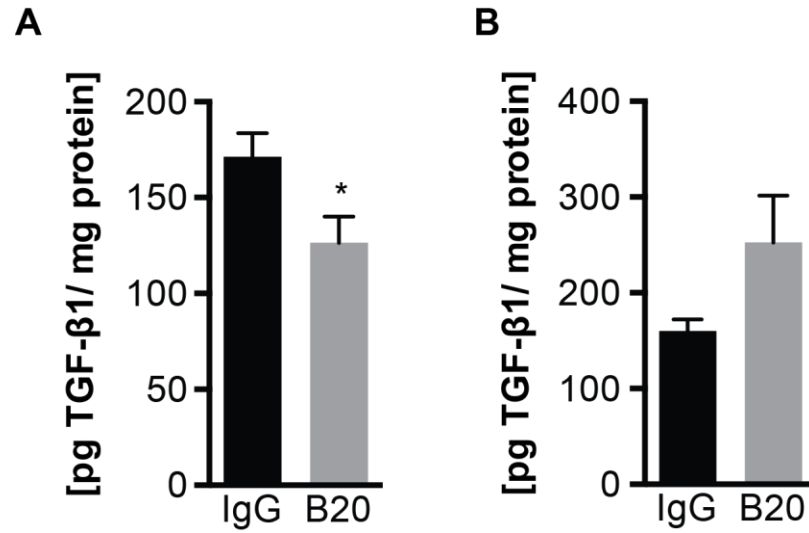


Fig. S9: Anti-VEGF therapy does not increase TGF-β1 expression in CRC liver metastases. Quantification of TGF-β1 protein concentration by ELISA in SL4 ($*P = 0.028$, Student's t-test, $n = 8/\text{group}$) and CT26 ($*P = 0.15$, Student's t-test, $n = 5-7/\text{group}$) liver metastases after treatment with IgG or B20 (5 mg/kg) for 6 days (treatments on day 0 and day 3).

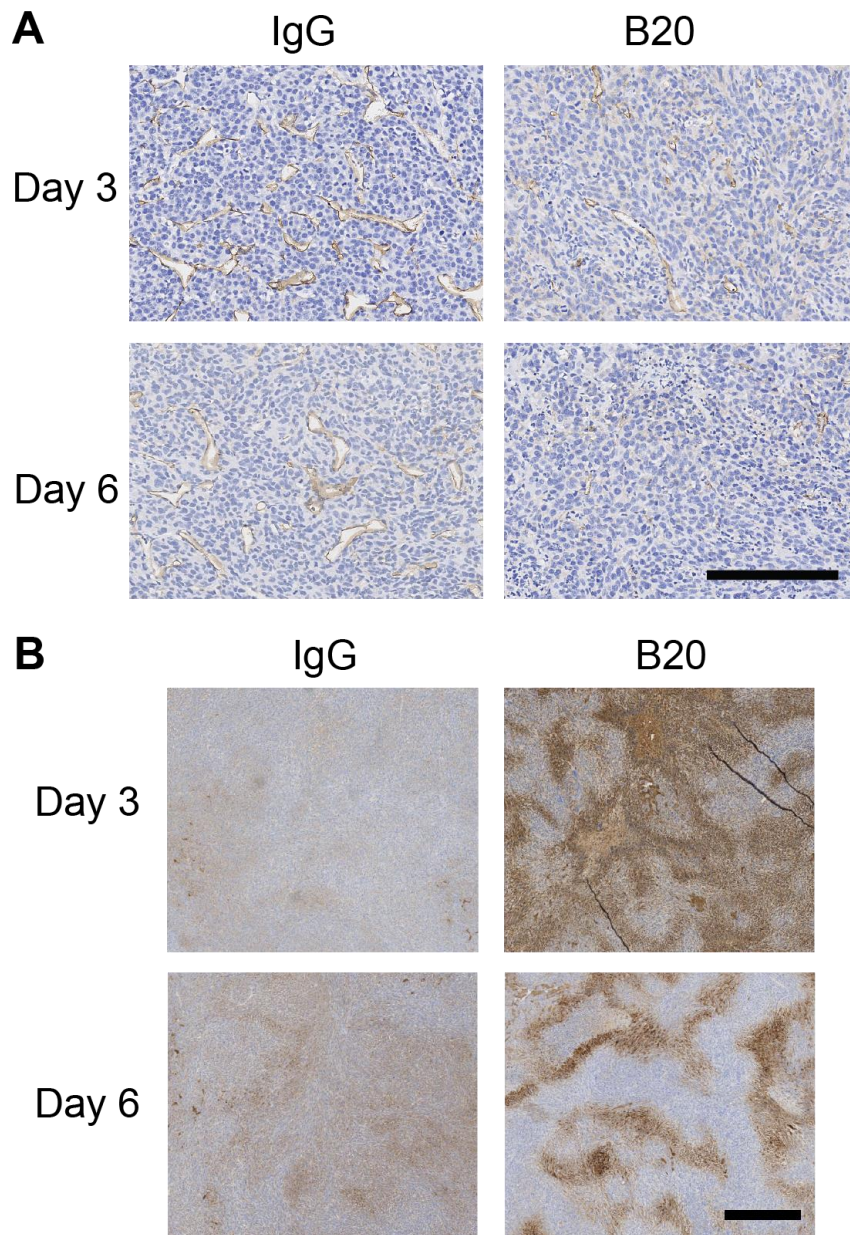


Fig. S10: Microvessel density is decreased, and hypoxia is increased in CT26 liver metastases after anti-VEGF therapy. (A) Representative immunohistochemistry images of microvessel density (CD34 staining) of CT26 liver metastases grown in BALB/c mice after 3 and 6 days of treatment with IgG or B20 (B) Representative immunohistochemistry images of hypoxic area fraction (pimonidazole adduct staining) of CT26 liver metastases grown in BALB/c mice after 3 and 6 days of treatment with IgG or B20. B20 treatments (5 mg/kg): on day 0 for 3-day experiments; on day 0 and day 3 for 6-day experiments. Scale bars for A and B, 100 μ m.

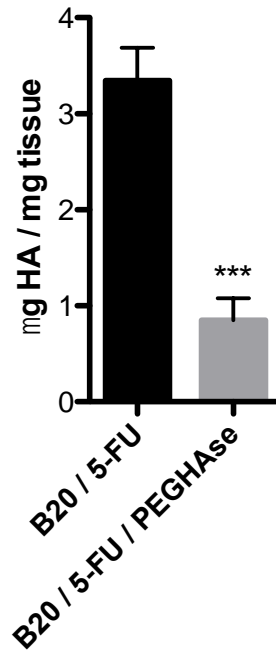


Fig. S11: Treatment with PEG-HAse lowers HA content in SL4 liver metastases. Quantification of HA concentration in SL4 liver metastases after treatment with B20 (5 mg/kg, twice a week) and 5-FU (50 mg/kg, twice a week) with and without PEG-HAse (4.5 mg/kg, twice a week) ($***P = 0.0007$, Student's t-test).

Table S1: Clinicopathologic data of patients with CRC liver metastases.

	No preoperative chemotherapy	Preoperative chemotherapy	Preoperative chemotherapy + bevacizumab
n	17	15	17
Gender			
Male	9 (52.9)	10 (66.7)	10 (58.8)
Female	8 (47.1)	5 (33.3)	7 (41.2)
Age	59 (2.5)	60 (2.4)	52 (2.4)
Site of primary			
Colon	11 (64.7)	8 (53.3)	10 (58.8)
Rectum	6 (35.3)	7 (46.7)	7 (41.2)
T category of primary			
T1/2	4 (23.5)	1 (6.7)	0 (0)
T3/4	13 (76.5)	14 (93.3)	17 (100)
N category of primary			
N0	10 (58.8)	2 (13.3)	6 (35.3)
N1/2	7 (41.2)	13 (86.7)	11 (64.7)
Histological grading of primary	13 (76.5)	9 (60.0)	9 (52.9)
Good/moderate differentiation	4 (23.5)	6 (40.0)	8 (47.1)
Poor differentiation			
Time of metastasis			
Synchronous	7 (41.2)	10 (66.7)	14 (82.3)
Metachronous	10 (58.8)	5 (33.3)	3 (17.7)
Multiple metastases	9 (52.9)	11 (73.3)	12 (70.6)
Size of metastasis \geq 5 cm	3 (17.7)	4 (26.7)	4 (23.5)
Bilobar metastases	6 (35.3)	8 (53.3)	6 (35.3)
Chemotherapy regimen			
FOLFOX	-	5 (33.3)	7 (41.2)
FOLFIRI	-	10 (66.7)	10 (58.8)
Number of chemotherapy cycles	-	6.3 (1.1)	7.0 (0.8)

Data are presented for 49 liver resections performed in 43 patients. Data are shown as mean (SEM) or n (%)